

1 **Supporting information for:**

2

3 *In vitro* biotransformation of pharmaceuticals and pesticides by  
4 trout liver S9 in the presence and absence of carbamazepine

5 *Junho Jeon*<sup>a, b, c\*</sup> and *Juliane Hollender*<sup>c, d</sup>

6

7 <sup>a</sup> Graduate School of FEED of Eco-Friendly Offshore Structure, Changwon National  
8 University, Changwon, Gyeongsangnamdo, 51140, Korea

9 <sup>b</sup> School of civil, environmental and chemical engineering, Changwon National  
10 University, Changwon, Gyeongsangnamdo, 51140, Korea

11 <sup>c</sup>Eawag, Swiss Federal Institute of Aquatic Science and Technology, 8600 Dübendorf,  
12 Switzerland

13 <sup>d</sup> Institute of Biogeochemistry and Pollutant Dynamics, ETH Zürich, CH-8092, Zürich,  
14 Switzerland

15

16 \* Corresponding author: Junho Jeon

17 Tel: +82 55 213 3748

18 Fax: +82 55 281 3011

19 E-mail: jjh0208@changwon.ac.kr

20

21	<b>Table of contents</b>	
22	Table S1. Physico-chemical properties of target compounds	<b>S3</b>
23	Table S2. Information on suppliers and purity/grade for used chemicals	<b>S4</b>
24	Table S3. Predicted biotransformation reactions and the resulting changes in molecular	
25	formula and exact mass occurring at parent compounds (Carbamazepine (CMZ),	
26	Azoxystrobin (AZX), Diazinon (DIZ), Fipronil (FPN), and Propranolol (PRN))	<b>S5</b>
27	Table S4. Time program of HPLC gradient for mobile and loading phase.	<b>S6</b>
28	Table S5. Adjusted conversion factors calculated by two regression models to estimate	
29	log IE based on physic-chemical properties (pKa and log (molecular volume)) and	
30	chromatographic retention time.	<b>S7</b>
31	Table S6. Parameters used in SIEVE 2.1 for comparative analysis over two different raw	
32	data sets to identify non-targeted metabolites.	<b>S8</b>
33	SI A. Setting parameters for ionization and data acquisition in QExactive	<b>S9</b>
34	Table S7. Recovery, limit of detection (LOD), and limit of quantification (LOQ) of	
35	parent compounds and metabolites with S9 matrix for online-SPE-Orbitrap method	<b>S10</b>
36	Figure S1. Variation of propranolol concentrations in active S9 fraction and heat-treated	
37	control	<b>S11</b>
38	Figure S2. Extracted ion chromatograms of propranolol and its metabolites with retention	
39	time and normalized largest peak intensity (NL)	<b>S12</b>
40	Figure S3. MS/MS spectra for carbamazepine (a) and its metabolites (b).	<b>S13</b>
41	Figure S4. MS/MS spectra for azoxystrobin (a) and its metabolites (b)~(c).	<b>S14</b>
42	Figure S5. MS/MS spectra for diazinon (a) and its metabolites (b)~(c).	<b>S15</b>
43	Figure S6. MS/MS spectra for fipronil (a) and its metabolites (b)~(c).	<b>S16</b>
44	Figure S7. Linear increase in formation of metabolites over incubation time (up to 60 min)	
45	<b>S17</b>	
46	Figure S8. Ratio of metabolite amount to the parent, diazinon with increasing	
47	carbamazepine concentration.	<b>S18</b>
48	Figure S9. Formation of MDI1 and MDI2 at different S9 protein concentrations after 30	
49	min incubation.	<b>S19</b>
50	References	<b>S20</b>
		<b>S2</b>

51 Table S1. Physico-chemical properties of target compounds

52

<i>Target compounds</i>	<i>Specific classification</i>	<i>CAS #</i>	<i>Formula</i>	<i>Exact mass</i>	<i>logK<sub>ow</sub>*</i>	<i>ISTD**</i>
Carbamazepine (CMZ)	Antiepileptic	298-46-4	C <sub>15</sub> H <sub>12</sub> N <sub>2</sub> O	236.0944	2.8	Carbamazepin-C13,D2
Azoxystrobin (AZX)	Fungicide	131860-33-8	C <sub>22</sub> H <sub>17</sub> N <sub>3</sub> O <sub>5</sub>	403.1163	4.2	Azoxystrobin-d4
Diazinon (DIZ)	Insecticide	333-41-5	C <sub>12</sub> H <sub>21</sub> N <sub>2</sub> O <sub>3</sub> PS	304.1005	4.2	Diazinon-D10
Fipronil (FPN)	Insecticide	120068-37-3	C <sub>12</sub> H <sub>4</sub> C <sub>12</sub> F <sub>6</sub> N <sub>4</sub> OS	435.9387	4.5	Diclofenac-D4
Propranolol (PRN)	Beta-blocker	525-66-6	C <sub>16</sub> H <sub>21</sub> NO <sub>2</sub>	259.1567	2.6	Propranolol-D7

53 \* estimated by MarvinSketch Ver. 5.10.3, \*\*Isotope-labelled internal standard for quantification of parent compounds and their  
 54 metabolites

55 Table S2. Information on suppliers and purity/grade for used chemicals

56

<b>Compound</b>	<b>Supplier</b>	<b>Remarks</b>
Carbamazepine (CMZ)	Toronto Research Chemicals Inc.	98.4 %
Azoxystrobin (AZX)	Toronto Research Chemicals Inc.	> 98 %
Diazinon (DIZ)	Dr. Ehrenstorfer GmbH	> 99 %
Fipronil (FPN)	Sigma-Aldrich Co. LLC	98 %
Propranolol (PRN)	Toronto Research Chemicals Inc.	98.7 %
Carbamazepin-10,11-epoxid (MCM)	Toronto Research Chemicals Inc.	> 99 %
Azoxystrobin acid (MAZ1)	HPC Standards GmbH	99 %
Diazoxon (MDI1)	Dr. Ehrenstorfer GmbH	> 98 %
Pyrimidinol (MDI2)	Sigma-Aldrich Co. LLC	99 %
Fipronil-sulfide (MFP1)	Dr. Ehrenstorfer GmbH	> 99%
Fipronil-sulfon (MFP2)	Dr. Ehrenstorfer GmbH	> 98 %
Carbamazepin-C13,D2	Dr. Ehrenstorfer GmbH	> 98 %
Azoxystrobin-d4	Sigma-Aldrich Co. LLC	98 %
Diazinon-D10	Dr. Ehrenstorfer GmbH	> 98 %
Diclofenac-D4	Toronto Research Chemicals Inc.	> 98 %
Propranolol-D7	Toronto Research Chemicals Inc.	> 98 %
Ammonium acetate	Merck	Analytical grade
Calcium chloride	Sigma-Aldrich Co. LLC	Analytical grade
Formic acid	Acros Organics	HPLC grade
$\beta$ -Nicotinamide adenine dinucleotide phosphate (NADPH), reduced tetra salt	Sigma-Aldrich GmbH	> 95 %
Ethylenediaminetetraacetic acid disodium salt dihydrate (EDTA)	Sigma-Aldrich GmbH	> 99%
Trout Liver S9 Homogenate	Life Technology (Basel, CH)	20 mg protein/ml
Bovine Serum Albumin	Sigma	> 96%
Water	Acros Organics	HPLC grade
Methanol	Acros Organics	HPLC grade
Acetonitrile	Acros Organics	HPLC grade

57

58 Table S3. Predicted biotransformation reactions and the resulting changes in molecular  
 59 formula and exact mass occurring at parent compounds (Carbamazepine (CMZ),  
 60 Azoxystrobin (AZX), Diazinon (DIZ), Fipronil (FPN), and Propranolol (PRN))

	<b>reactions</b>	<b>loss</b>	<b>gain</b>	<b><math>\Delta</math>mass</b>	<b>Parent compound</b>
<b>Universal</b>	Hydroxylation, N/S-Oxidation, or Epoxidation		O	+15.9949	
	Demethylation	CH <sub>2</sub>		-14.0157	
	Dehydrogenation	H <sub>2</sub>		-2.0157	
	Hydrogenation		H <sub>2</sub>	+2.0157	
<b>Structure specific</b>	Oxidative displacement of amine	NH <sub>2</sub>	OH	+0.9840	CMZ,
	N-Dealkylation1	CH <sub>2</sub> NO	H	-43.0058	CMZ
	O-Dealkylation1	C <sub>7</sub> H <sub>4</sub> N	H	-101.0266	AZX
	O-Dealkylation2	C <sub>11</sub> H <sub>6</sub> N <sub>3</sub> O	H	-195.0433	AZX
	O-Dealkylation3	C <sub>2</sub> H <sub>4</sub>		-28.0313	DIZ
	O-Dealkylation4	C <sub>4</sub> H <sub>8</sub>		-56.0626	DIZ
	O-Dealkylation5	C <sub>4</sub> H <sub>10</sub> O <sub>2</sub> PS	H	-152.0061	DIZ
	S-Dealkylation1	CF <sub>3</sub>	H	-67.9874	FPN
	N-Dealkylation2	C <sub>7</sub> H <sub>2</sub> F <sub>3</sub> Cl <sub>2</sub>	H	-211.9407	FPN
	O-Dealkylation6	C <sub>6</sub> H <sub>13</sub> NO		-115.0997	PRN
	Deisopropylation	C <sub>3</sub> H <sub>6</sub>		-42.0470	PRN

61  
 62  
 63  
 64  
 65  
 66  
 67

68 Table S4. Time program of HPLC gradient for mobile and loading phase.  
69

Separation	Time (min)	H <sub>2</sub> O (μL/min)	MeOH (μL/min)
Mobile phase	0.00	40	260
	4.00	40	260
	14.00	280	20
	26.00	280	20
	26.20	40	260
	32.30	40	260
Enrichment	Time (min)	2mM ammonium acetate* (μL/min)	Acetonitrile** (μL/min)
Loading phase	0.00	200	0
	0.10	0	2000
	0.60	0	2000
	0.65	2000	0
	5.60	2000	0
	5.65	400	0
	6.20	400	0
	6.30	0	400
	9.90	0	400
	10.00	400	0
	20.60	400	0
	20.70	2000	0
	32.00	2000	0
	32.10	200	0

70 \*ammonium acetate solution was used for loading online sample, \*\*acetonitrile was used  
71 for cleaning line, loop, and SPE cartridge where the sample passes through.

72 Table S5. Adjusted conversion factors calculated by two regression models to estimate  
 73 log IE based on physic-chemical properties (pKa and log (molecular volume)) and  
 74 chromatographic retention time.  
 75

<i>Molecules</i>	<i>Conversion factor *</i>	<i>Adjusting factor**</i>	<i>Adjusted conversion factor***</i>
Propranol	1.00	1.00	1.00
MPR218	0.32	0.94	0.30
MPR276A	0.53	0.83	0.44
MPR276B	1.12	1.12	1.25

76 \*Relative IE of BTP to the parent calculated by the multivariable regression model  
 77 (pka/MV vs IE, equation (1)-(3) in SI of Jeon et al. (Jeon et al., 2013)), \*\* Relative IE of  
 78 BTP to the parent calculated by the linear regression curves (retention time vs IE, shown  
 79 in Figure S4 in SI of Jeon et al. (Jeon et al., 2013) ) , \*\*\* Adjusted conversion factor =  
 80 conversion factor x adjusting factor  
 81  
 82  
 83  
 84

85 Table S6. Parameters used in SIEVE 2.1 for comparative analysis over two different raw  
 86 data sets to identify non-targeted metabolites.  
 87

Alignment parameters		Frame parameters		Identification parameters	
AlignmentBypass	False	FrameFromMS2	False	Adduct	M+H
AlignmentMinIntensity	1000	MaximumFrames	20000	AccumedCharge	1
CorrelationBinWidth	1	MZStart	150	ChemSpiderDBs	KEGG
RTLimitsForAlignment	True	MZStop	600	FrameIDCriteria	Order by P value
TileIncrement	150	MZWidth	0.02	MaximumIDs	1000
TileMaximum	300	PRMaxCharge	5	MZTolerance	0.02
TileSize	300	RTStart	10-14	RandomSeed	12345
TileThreshold	0.6	RTStop	18-20	SearchSource	SEQUEST
		RTWith	2.5	UserPercolator	False
		Threshold	5000		

88



89 ***SI A. Setting parameters for ionization and data acquisition in QExactive***  
90  
91 Detection of analytes was performed with the QExactive using electrospray ionization  
92 (ESI) interface in positive and negative mode (Q Exactive Orbitrap LC-ESI-MS/MS,  
93 Thermo Fisher Scientific Inc.). The spray voltage was +4000 V (positive mode) or -3000  
94 V (negative mode), the capillary temperature was held at 350 °C, S-lens-level was set at  
95 50 (default value, numerical factor from 0-100), the auxiliary gas flow rate was 15 L/min,  
96 and the sheath gas flow rate was 40 L/min for both ionization modes. A mass range from  
97 100 - 1000 m/z was analyzed in full scan with a maximal ion count of 1,000,000.  
98 External mass calibration was used to ensure a mass accuracy of < 3 ppm over the mass  
99 range. The QExactive operation method was designed to perform data-dependent MS/MS  
100 for the five most intense ions among the mass list of parents and BTPs for each scan  
101 event. During the MS/MS acquisition, 'dynamic exclusion' function was simultaneously  
102 applied to prevent an ion from triggering a subsequent data-dependent MS/MS scan for a  
103 pre-selected length of time (we chose 3 sec) after it has already triggered a data-  
104 dependent MS/MS scan. If no mass from the list of predicted BTPs was found, the most  
105 intense ions were fragmented. Optimum collision energy for MS/MS fragmentation in the  
106 higher energy collision dissociation (HCD) was estimated by an empirical linear equation  
107 which is a function of exact mass. High-resolution mass spectra with a resolution of  
108 70,000 and a mass accuracy of <3 ppm were recorded. Data-dependent MS/MS  
109 acquisition at a resolution of 35,000 was triggered at each scan event. Data were analyzed  
110 with Xcalibur (Thermo Scientific, USA) in the Qual Browser for identification.  
111  
112

Table S7. Recovery, limit of detection (LOD), and limit of quantification (LOQ) of parent compounds and metabolites with S9 matrix for online-SPE-Orbitrap method

Target compounds	Recovery* (%)	LOQ** (pg/mL)
Carbamazepine (CMZ)	118	0.1
Azoxystrobin (AZX)	100	0.5
Diazinon (DIZ)	105	0.5
Fipronil (FPN)	85	5.0
Propranolol (PRN)	128	0.1
Carbamazepin-10,11-epoxid (MCM)	75	0.5
Azoxystrobin acid (MAZ1)	88	0.5
Diazoxon (MDI1)	60	1.0
Pyrimidinol (MDI2)	80	0.1
Fipronil-sulfide (MFP1)	75	1.0
Fipronil-sulfon (MFP2)	70	5.0

\* Recovery of whole sample treatment procedure for S9 matrix (injection amount : 2 ng for the parents, 0.1 for the metabolites), \*\*Limit of quantification for online SPE-Orbitrap method, defined as concentration yielding 10 times greater than signal to noise

Figure S1. Variation of propranolol concentrations in active S9 fraction and heat-treated control. (Error bars indicate standard deviation between replicates, n=3)

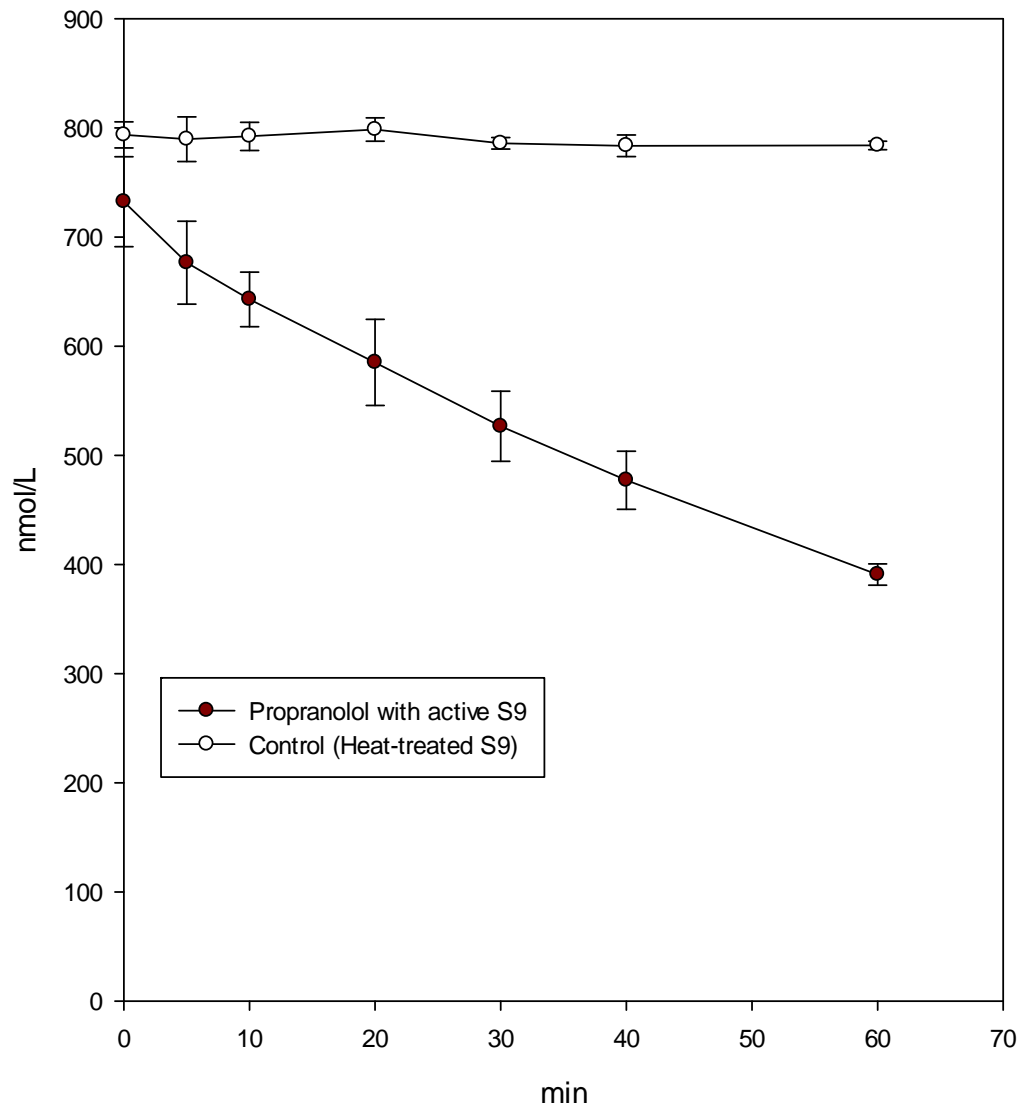


Figure S2. Extracted ion chromatograms of propranolol and its metabolites with retention time and normalized largest peak intensity (NL)

RT: 9.95 - 14.53

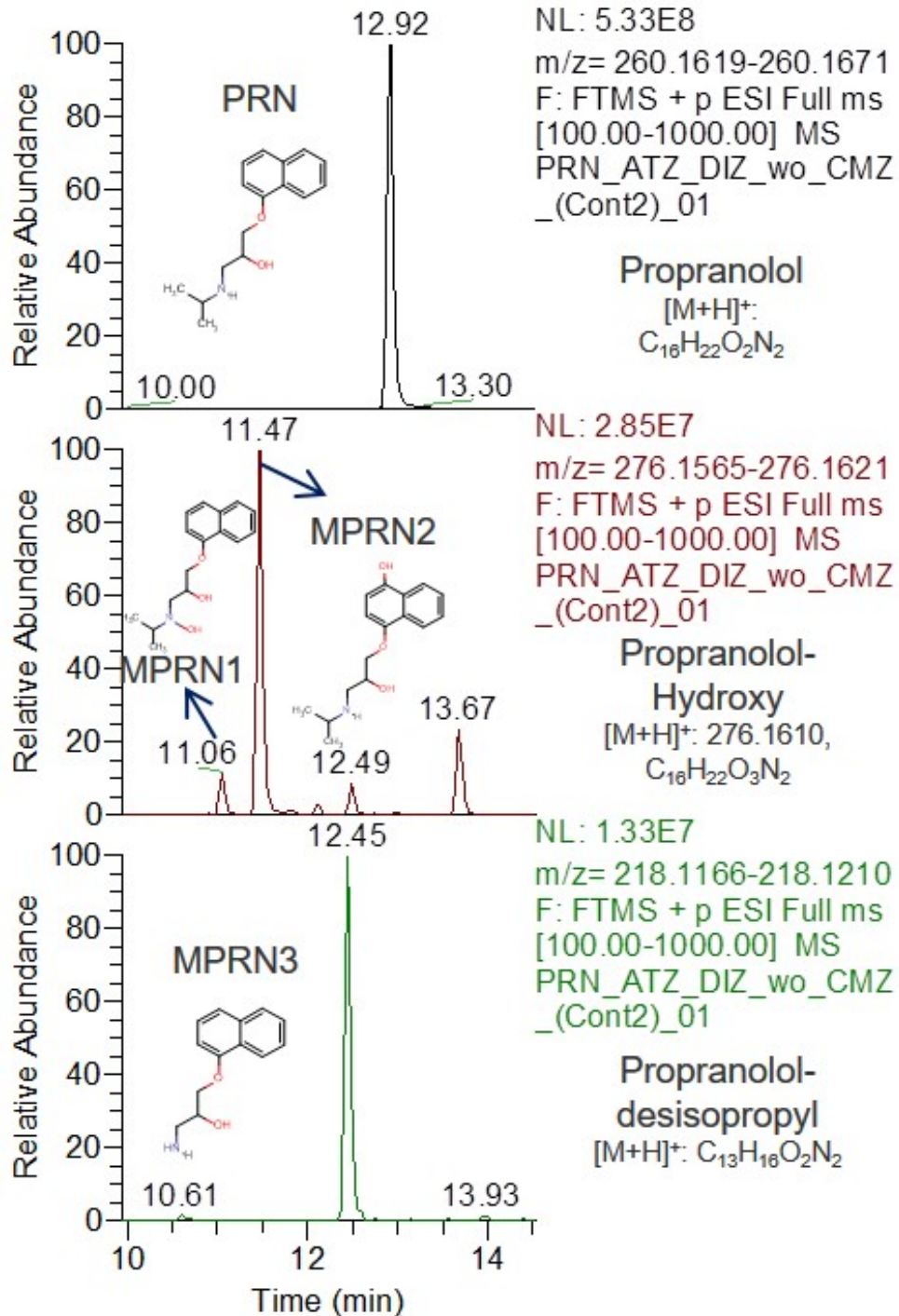
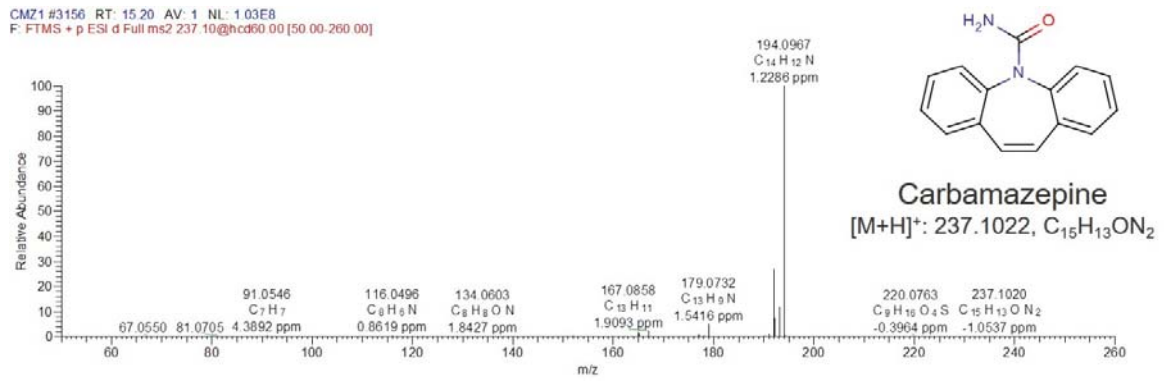


Figure S3. MS/MS spectra for carbamazepine (a) and its metabolites (b).

(a)



(b)

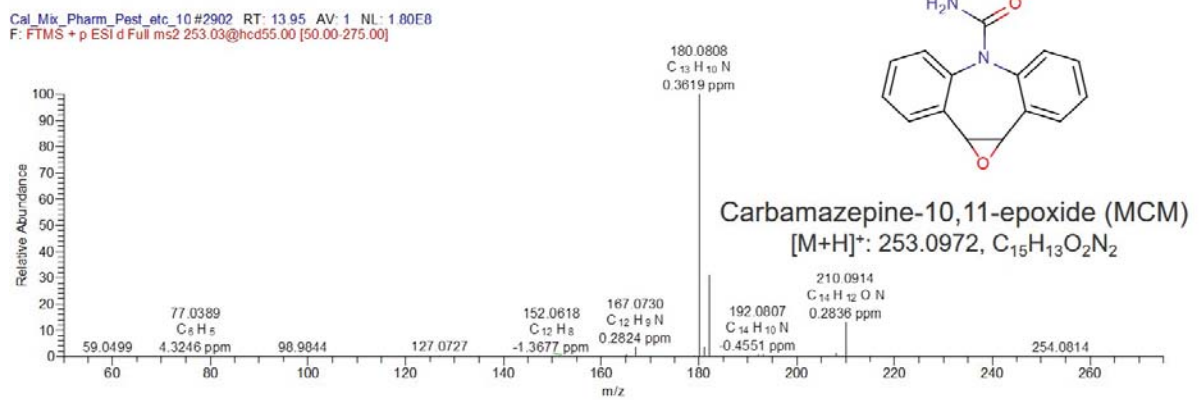
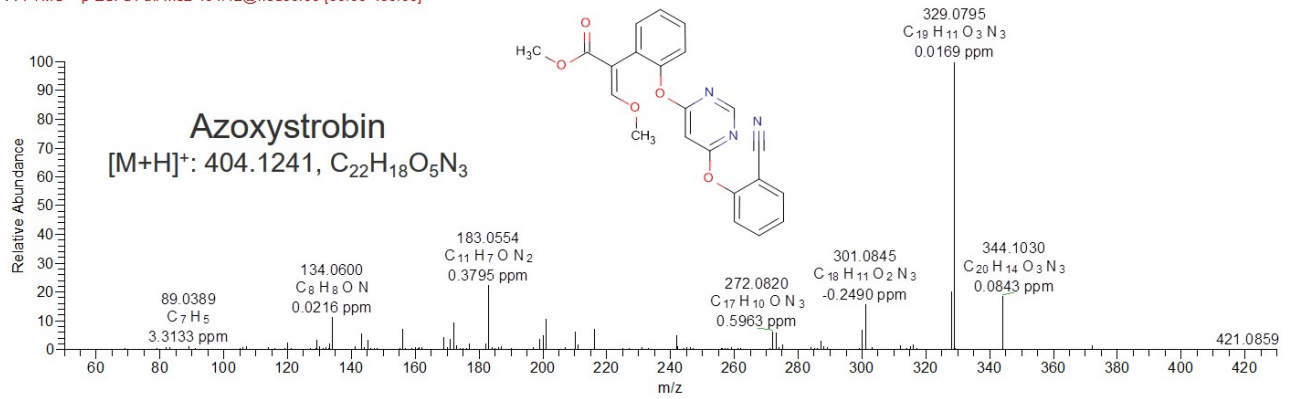


Figure S4. MS/MS spectra for azoxystrobin (a) and its metabolites (b)~(c).

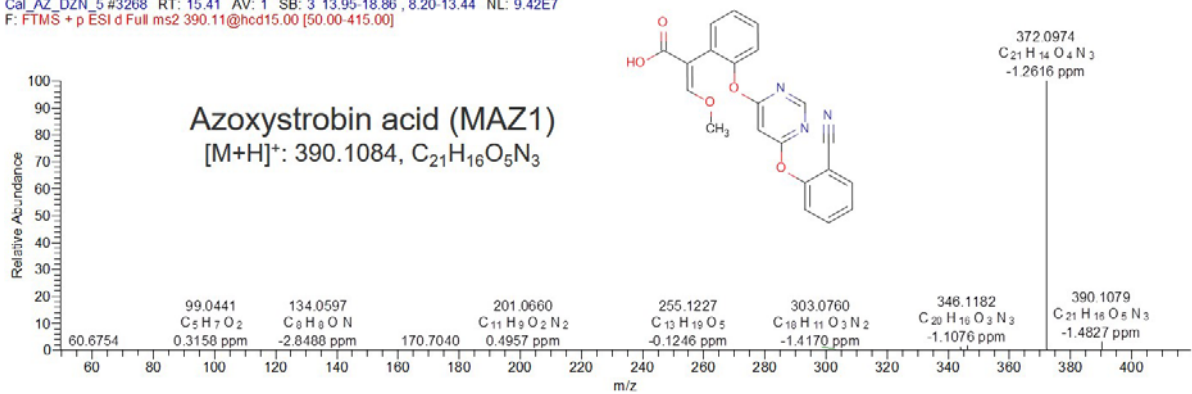
(a)

PRN\_AZ\_DIZ\_FPN\_without\_CMZ\_Cont2\_03 #3316 RT: 15.90 AV: 1 NL: 1.19E8  
F: FTMS + p ESI d Full ms2 404.12@hcd50.00 [50.00-430.00]



(b)

Cal\_AZ\_DZN\_5 #3268 RT: 15.41 AV: 1 SB: 3 13.95-18.86, 8.20-13.44 NL: 9.42E7  
F: FTMS + p ESI d Full ms2 390.11@hcd15.00 [50.00-415.00]



(c)

AZX\_without\_CMZ #1973 RT: 15.58 AV: 1 SB: 16 13.95-18.87, 9.29-13.44 NL: 2.07E4  
F: FTMS + p ESI Full ms2 362.11@hcd15.00 [50.00-390.00]

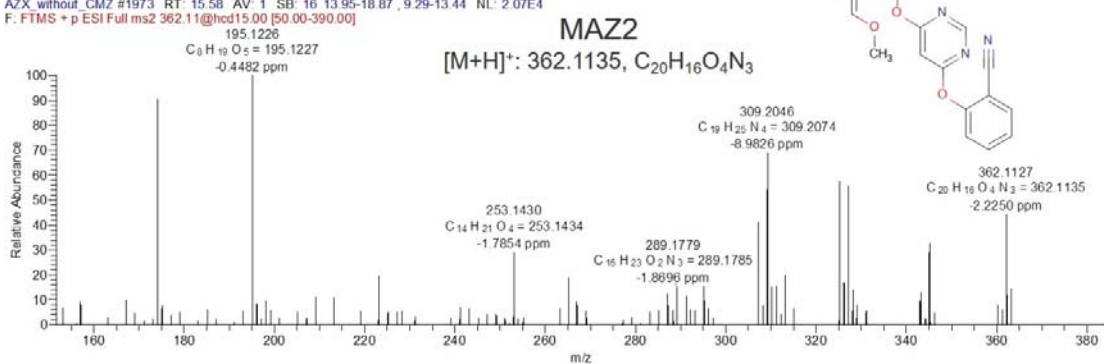
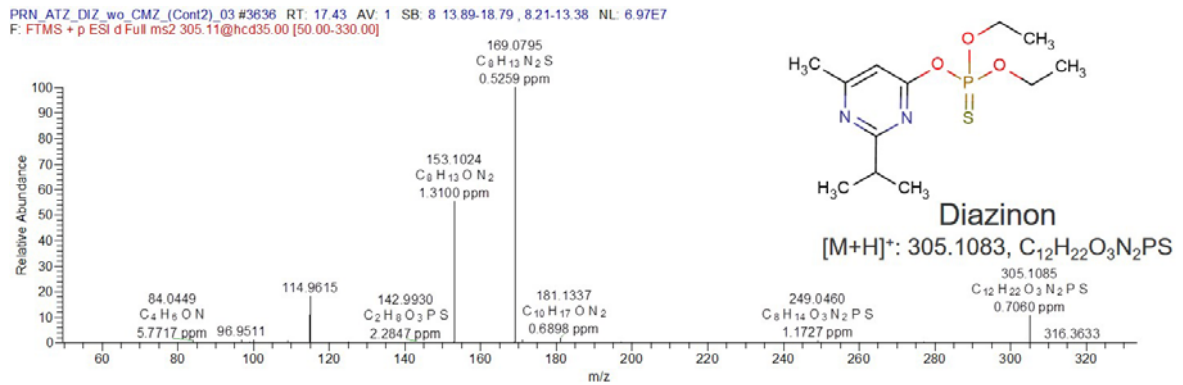
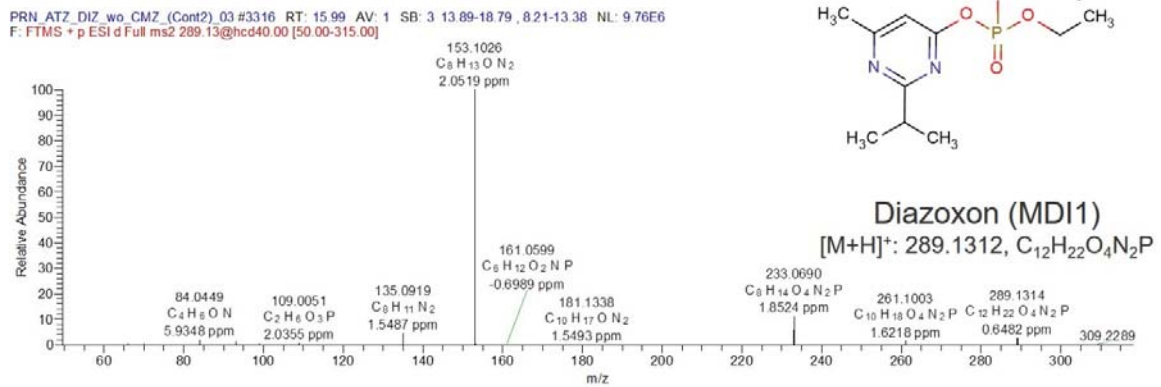


Figure S5. MS/MS spectra for diazinon (a) and its metabolites (b)~(c).

(a)



(b)



(c)

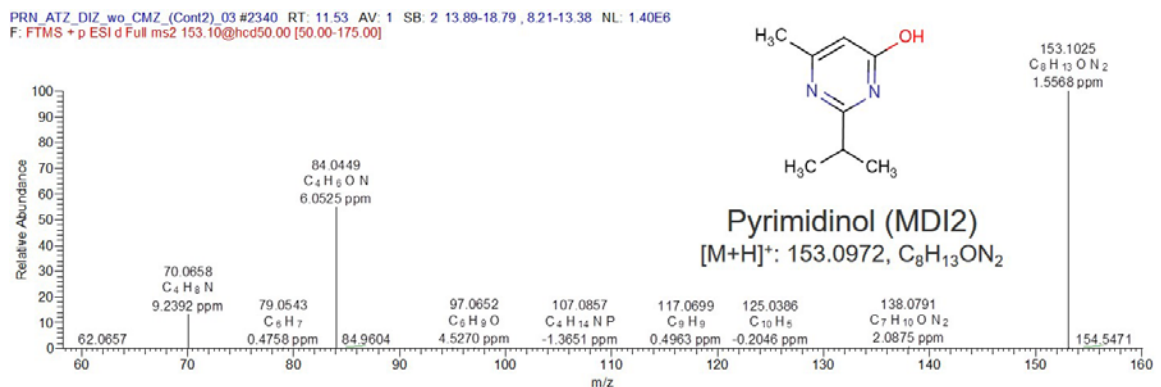
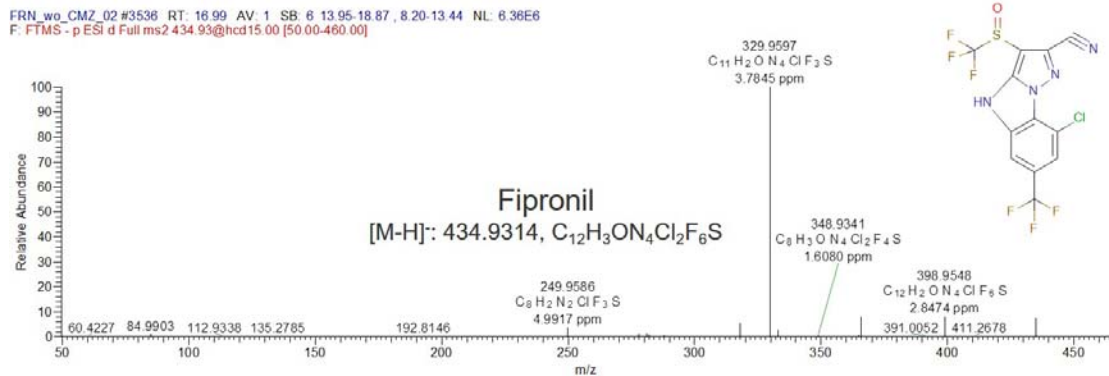
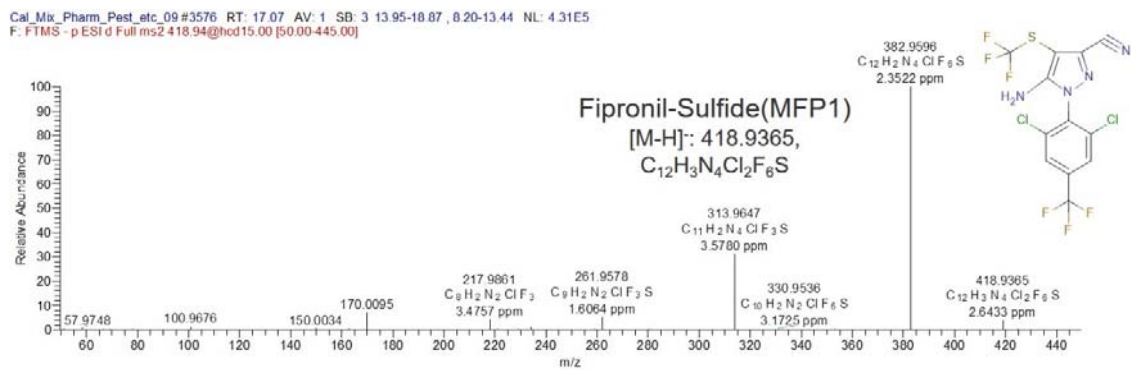


Figure S6. MS/MS spectra for fipronil (a) and its metabolites (b)~(c).

(a)



(b)



(c)

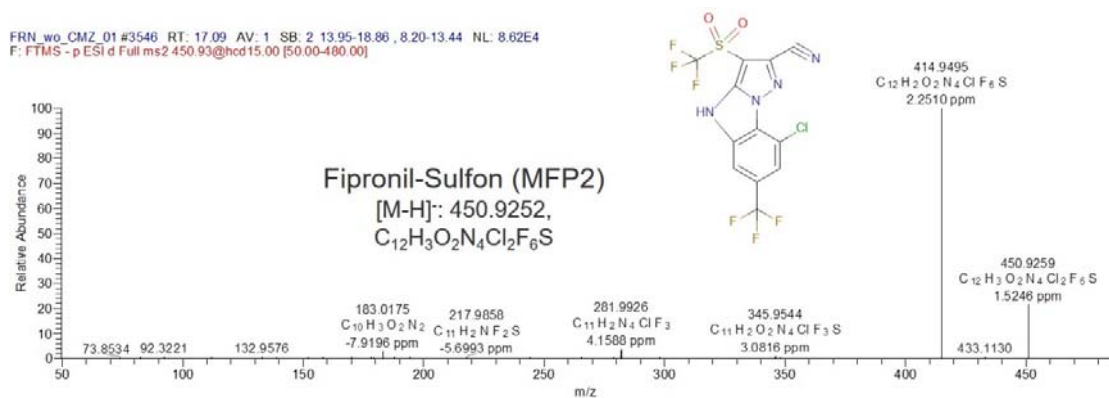




Figure S7. Linear increase in formation of metabolites over incubation time up to 60 min (Error bars indicate standard deviation between replicates, n=3)

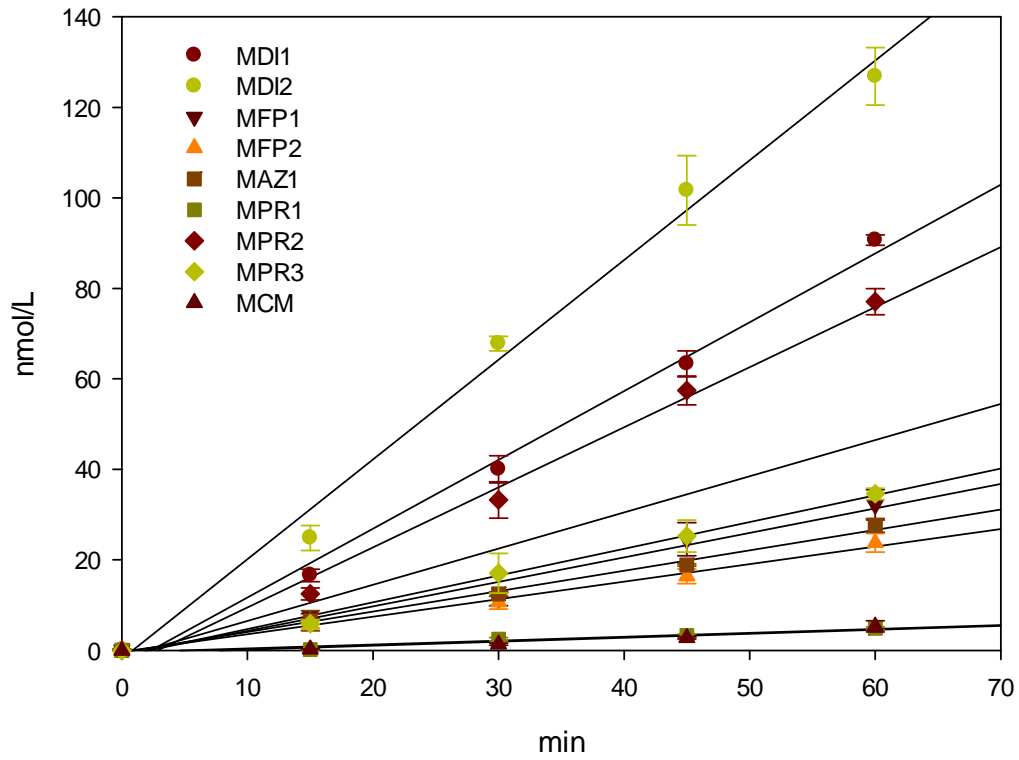


Figure S8. Ratio of metabolite amount to the parent, diazinon with increasing carbamazepine concentration. (Error bars indicate standard deviation between replicates, n=3)

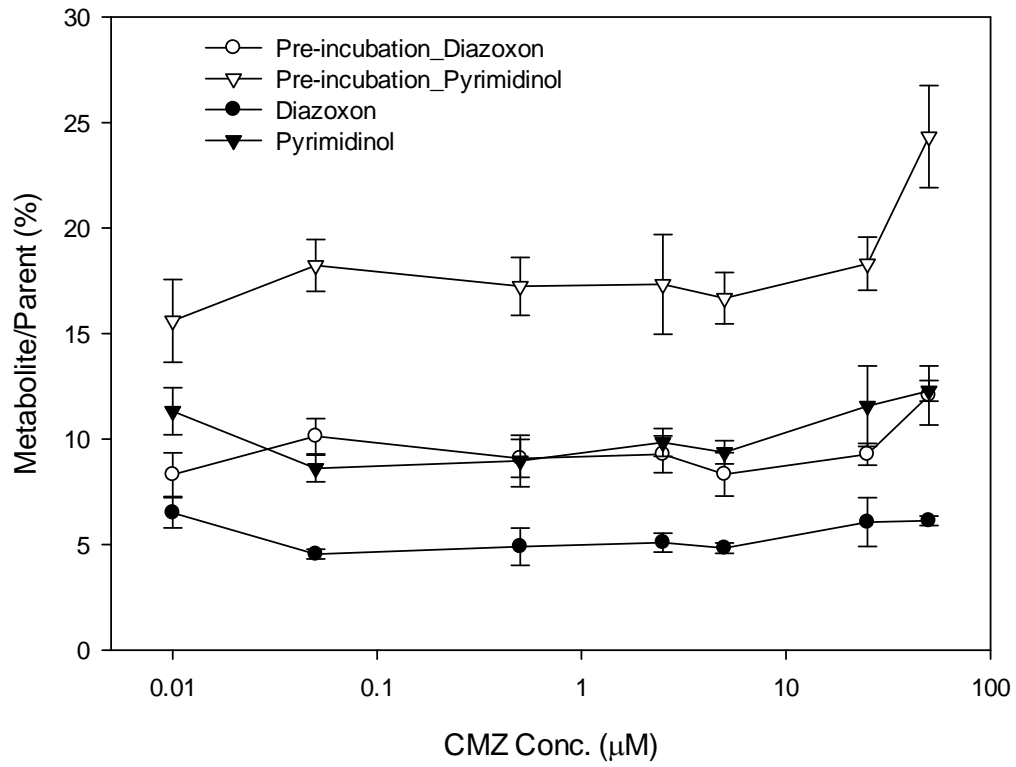
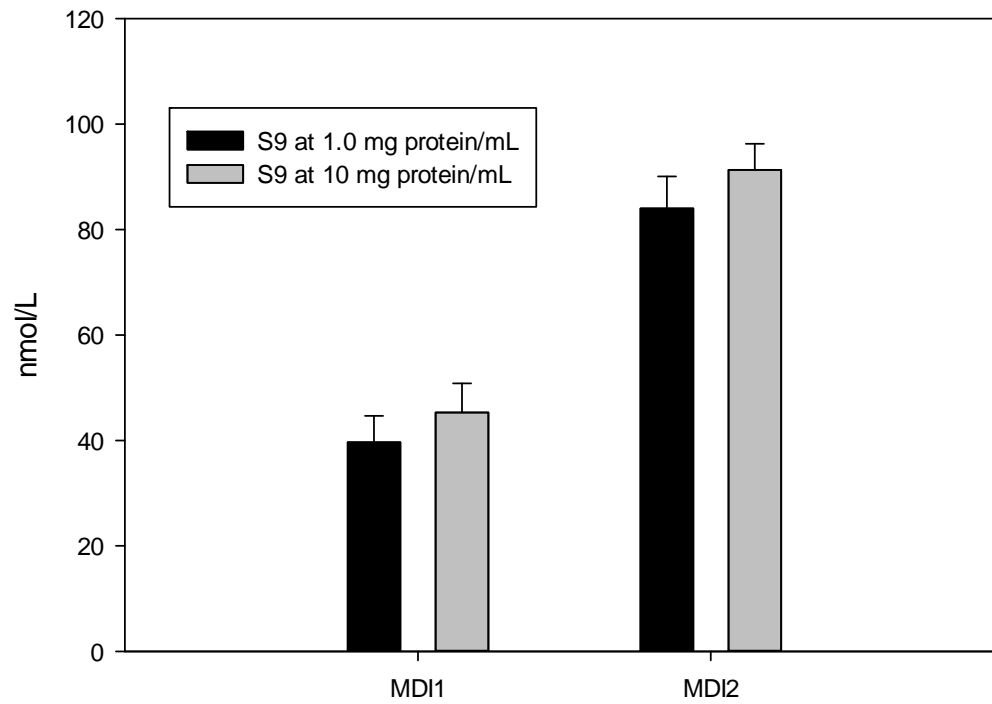


Figure S9. Formation of MDI1 and MDI2 at different S9 protein concentrations after 30 min incubation. (Error bars indicate standard deviation between replicates, n=3)



## *References*

- Jeon, J., Kurth, D., Ashauer, R., Hollender, J., 2013. Comparative toxicokinetics of organic micropollutants in freshwater crustaceans. *Environ. Sci. Technol.* 47.  
doi:10.1021/es400833g